Inorg. Chem. **2005**, *44*, 2815–2825

Reactions of the Dianion [1,1,1-(CO)$_3$-2-Ph-*closo*-1,2-MnCB$_9$H$_9$]$^{2-}$ with Transition-Metal Cations: Facile Insertion and Then Extrusion of Cluster Vertexes

Shaowu Du,[†] John C. Jeffery,[‡] Jason A. Kautz,[†] Xiu Lian Lu,[†] Thomas D. McGrath,[†] Thomas A. Miller,[‡] T. Riis-Johannessen,[‡] and F. Gordon A. Stone*[,†]

Department of Chemistry & Biochemistry, Baylor University, Waco, Texas 76798-7348, and School of Chemistry, University of Bristol, Bristol BS8 1TS, U.K.

Received November 22, 2004

The manganacarborane dianion in [N(PPh$_3$)$_2$][NEt$_4$][1,1,1-(CO)$_3$-2-Ph-*closo*-1,2-MnCB$_9$H$_9$] (**1b**) reacts with cationic transition metal–ligand fragments to give products in which the electrophilic metal groups (M′) are exo-polyhedrally attached to the {*closo*-1,2-MnCB$_9$} cage system via three-center two-electron B–H → M′ linkages and generally also by Mn–M′ bonds. With {Cu(PPh$_3$)}$^+$, the Cu–Mn–Cu trimetallic species [1,6-{Cu(PPh$_3$)}-1,7-{Cu(PPh$_3$)}-6,7-(μ-H)$_2$-1,1,1-(CO)$_3$-2-Ph-*closo*-1,2-MnCB$_9$H$_7$] (**3a**) is formed, whereas reactions with {M′(dppe)}$^{2+}$ (M′ = Ni, Pd; dppe = Ph$_2$PCH$_2$CH$_2$PPh$_2$) give [1,3-{Ni(dppe)}-3-(μ-H)-1,1,1-(CO)$_3$-2-Ph-*closo*-1,2-MnCB$_9$H$_8$] (**5a**) and [1,3,6-{Pd(dppe)}-3,6-(μ-H)$_2$-1,1,1-(CO)$_3$-2-Ph-*closo*-1,2-MnCB$_9$H$_7$] (**5b**), both of which contain M′–Mn bonds. The latter reaction with M′ = Pt affords [3,6-{Pt(dppe)}-3,6-(μ-H)$_2$-1,1,1-(CO)$_3$-2-Ph-*closo*-1,2-MnCB$_9$H$_7$] (**6**), which lacks a Pt–Mn connectivity. Compound **6** itself spontaneously converts to [1-Ph-2,2,2-(CO)$_3$-8,8-(dppe)-*hypercloso*-8,2,1-PtMnCB$_9$H$_9$] (**7b**) and thence to [3,6,7-{Mn(CO)$_3$}-3,7-(μ-H)$_2$-1-Ph-6,6-(dppe)-*closo*-6,1-PtCB$_8$H$_6$] (**8**). This sequence occurs via initial insertion of the {Pt(dppe)} unit and then extrusion of {Mn(CO)$_3$} and one {BH} vertex. In the presence of alcohols ROH, compound **6** is transformed to the 7-OR substituted analogues of **7b**. X-ray diffraction studies were essential in elucidating the structures encountered in compounds **5**–**8** and hence in understanding their behavior.

Introduction

During the four decades since the discovery of metallacarboranes by Hawthorne and co-workers,[1] the field has been dominated by metal dicarbollide species and, in particular, by clusters with icosahedral {MC$_2$B$_9$} frameworks.[2] We have extended this area through studies of the corresponding metal monocarbollide {MCB$_{10}$} species, which have revealed compounds that are complementary to the dicarbollide systems, with some behaving similarly, but others displaying behavior unprecedented in metallacarborane chemistry.[3] In seeking to broaden further the scope of this work, we have begun to examine nonicosahedral species and have recently reported dianionic, 11-vertex rhenium and manganese monocarborane complexes, namely, the salts [N(PPh$_3$)$_2$][NEt$_4$]-[1,1,1-(CO)$_3$-2-Ph-*closo*-1,2-MCB$_9$H$_9$] [M = Re (**1a**),[4] Mn (**1b**)[5]]. The rhenium compound **1a** reacts with cationic transition-element fragments to afford carborane-supported polymetallic units that range from simple bimetallics,[4,6] through trimetallics having either V-shaped[4,6] or triangular[6] cores, to a unique {ReIrAu$_2$} "butterfly" species.[6] This

* To whom correspondence should be addressed. E-mail: gordon_stone@baylor.edu.
† Baylor University.
‡ University of Bristol.

(1) Hawthorne, M. F.; Young, D. C.; Wegner, P. A. *J. Am. Chem. Soc.* **1965**, *87*, 1818.
(2) (a) Grimes, R. N. In *Comprehensive Organometallic Chemistry*; Wilkinson, G., Abel, E. W., Stone, F. G. A., Eds.; Pergamon Press: Oxford, U.K., 1982; Vol. 1, Section 5.5. (b) Grimes, R. N. In *Comprehensive Organometallic Chemistry II*; Abel, E. W., Stone, F. G. A., Wilkinson, G., Eds.; Pergamon Press: Oxford, U.K., 1995; Vol. 1, Chapter 9. (c) Grimes, R. N. *Coord. Chem. Rev.* **2000**, *200*–*202*, 773.
(3) (a) McGrath, T. D.; Stone, F. G. A. *J. Organomet. Chem.* **2004**, *689*, 3891. (b) McGrath, T. D.; Stone, F. G. A. *Adv. Organomet. Chem.* **2005**, *53*, in press.
(4) Du, S.; Kautz, J. A.; McGrath, T. D.; Stone, F. G. A. *Organometallics* **2003**, *22*, 2842.
(5) Du, S.; Farley, R. D.; Harvey, J. N.; Jeffrey, J. C.; Kautz, J. A.; Maher, J. P.; McGrath, T. D.; Murphy, D. M.; Riis-Johannessen, T.; Stone, F. G. A. *Chem. Commun.* **2003**, 1846.
(6) Du, S.; Kautz, J. A.; McGrath, T. D.; Stone, F. G. A. *Angew. Chem., Int. Ed.* **2003**, *42*, 5728.

10.1021/ic048345w CCC: $30.25
Published on Web 03/12/2005

Chart 1

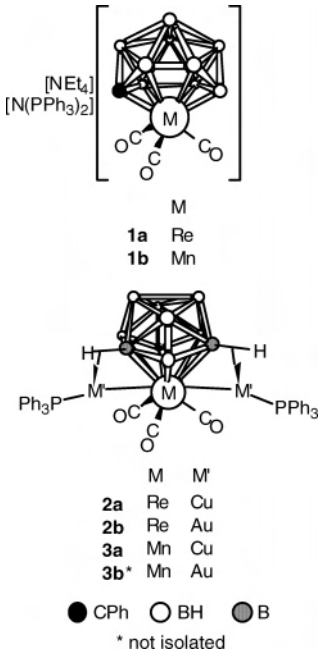

finding prompted the initiation of parallel studies of the reactivity of the manganese species **1b** with transition-metal cations. The results reported herein reveal some analogies with the chemistry of **1a**, but also some extraordinary differences.

Results and Discussion

When the rhenium complex **1a** is treated with sources of the cations $\{M'(PPh_3)\}^+$ (M′ = Cu, Au), the only metallacarborane products isolated—regardless of stoichiometry—are the trimetallic species [1,6-{M′(PPh$_3$)}-1,7-{M′(PPh$_3$)}-6,7-(μ-H)$_2$-1,1,1-(CO)$_3$-2-Ph-*closo*-1,2-ReCB$_9$H$_7$] [M′ = Cu (**2a**), Au (**2b**), Chart 1].[4] In parallel, reaction of the manganese complex **1b** with [CuCl(PPh$_3$)]$_4$ and Tl[PF$_6$] similarly gave a dicopper derivative, [1,6-{Cu(PPh$_3$)}-1,7-{Cu(PPh$_3$)}-6,7-(μ-H)$_2$-1,1,1-(CO)$_3$-2-Ph-*closo*-1,2-MnCB$_9$H$_7$] (**3a**, Chart 1), but the corresponding digold species **3b** (Chart 1) could not be isolated. It is known[5] that the dianion of compound **1b** is readily oxidized by HgCl$_2$, and conceivably, the $\{Au(PPh_3)\}^+$ cation affects **1b** similarly. Indeed, we have observed gold cluster species among the products of the reaction between **1b** and $\{Au(PPh_3)\}^+$, consistent with oxidation of the manganacarborane and a partial reduction of the gold reagent.[7]

Compound **3a** was characterized by the data presented in Tables 1−3. These data are broadly similar to those of **2a**,[4] but some significant differences are evident. Thus, for example, their $^{11}B\{^1H\}$ and $^{31}P\{^1H\}$ NMR spectra show similar chemical shifts and patterns, but the metal-bound CO ligands appear different in the two compounds. The latter groups give rise to a single broad resonance in the $^{13}C\{^1H\}$ NMR spectrum at δ 218.4 for **3a**, whereas two signals at δ 190.4 and 186.7 (2 × CO) are observed for **2a**. Likewise, the highest-frequency CO band in the IR spectrum of **3a** is at 2002 cm^{-1}, versus 2021 cm^{-1} for **2a**. However, the dianions of their parents **1b** and **1a**, respectively, show similar differences in their spectroscopic properties, and therefore, the apparent differences observed between compounds **3a** and **2a** might be attributable to the nature of the Mn versus Re centers, rather than to **3a** exhibiting a structure different from that of **2a**. Unfortunately, single crystals of **3a** suitable for an X-ray diffraction study were not available to confirm this hypothesis. The ^1H NMR spectrum of **3a** showed only resonances attributable to phenyl protons, with unfortunately no signals for the B−H → Cu protons; the latter would be useful in providing additional confirmation of the structure in the absence of an X-ray study. However, the resonances for such protons are rarely seen in ^1H NMR spectra because of extensive broadening by the adjacent quadrupolar Cu and B nuclei and by fluxional processes that are very rapid on the NMR time scale.[8] Nevertheless, the structure of **3a** is believed to be similar to that of **2a** on the basis of the spectral similarities discussed above. We note, moreover, in this connection that {M′(PPh$_3$)} derivatives (M′ = Cu, Ag, Au) of the related manganese and rhenium dicarbollide clusters [3,3,3-(CO)$_3$-*closo*-3,1,2-MC$_2$B$_9$H$_{11}$]$^-$ (M = Mn,[9] Re[10]) all have very similar architectures and, indeed, the Re−Cu, Re−Ag, Mn−Cu, and Mn−Au species are all crystallographically isomorphous.

The dianion of **1a** forms the bimetallic species [1,3-{M′(dppe)}-3-(μ-H)-1,1,1-(CO)$_3$-2-Ph-*closo*-1,2-ReCB$_9$H$_8$] [M′ = Ni (**4a**), Pd (**4b**), Pt (**4c**), Chart 2][4] with sources of the dications $\{M'(dppe)\}^{2+}$. All three of these compounds have similar NMR spectra and are believed to have similar molecular structures, with that of the Re−Pt derivative having been established by an X-ray diffraction study. The latter experiment showed the exo-polyhedral platinum fragment to be bonded to the rhenacarborane via a Re−Pt bond and one B−H → Pt agostic-type interaction, the latter involving the BH vertex in the γ position with respect to the carbon within the Re-bound CBB*B*BB belt. An additional long interaction to an adjacent β-BH was also noted. The dianion of **1b** behaves similarly to **1a** and also forms bimetallic complexes upon reaction with the same $\{M'(dppe)\}^{2+}$ dications. However, matters are rather more complicated in the present system; this is particularly so for the Mn−Pt case, which will therefore be discussed separately from the Ni and Pd species.

Reaction (18 h) of **1b** with [M′Cl$_2$(dppe)] (1 equiv) and Tl[PF$_6$] (2 equiv) in CH$_2$Cl$_2$ affords the complexes [1,3-{Ni(dppe)}-3-(μ-H)-1,1,1-(CO)$_3$-2-Ph-*closo*-1,2-MnCB$_9$H$_8$] (**5a**, Chart 2) and [1,3,6-{Pd(dppe)}-3,6-(μ-H)$_2$-

(7) Hall, K. P.; Mingos, D. M. P. *Prog. Inorg. Chem.* **1984**, *32*, 237.

(8) (a) Cabioch, J.-L.; Dossett, S. J.; Hart, I. J.; Pilotti, M. U.; Stone, F. G. A. *J. Chem. Soc., Dalton Trans.* **1991**, 519. (b) Batten, S. A.; Jeffrey, J. C.; Jones, P. L.; Mullica, D. F.; Rudd, M. D.; Sappenfield, E. L.; Stone, F. G. A.; Wolf, A. *Inorg. Chem.* **1997**, *36*, 2570. (c) Ellis, D. D.; Franken, A.; Jelliss, P. A.; Kautz, J. A.; Stone, F. G. A.; Yu, P.-Y. *J. Chem. Soc., Dalton Trans.* **2000**, 2509.

(9) Hata, M.; Kautz, J. A.; Lu, X. L.; McGrath T. D.; Stone, F. G. A. *Organometallics* **2004**, *23*, 3590.

(10) Ellis, D. D.; Jelliss, P. A.; Stone, F. G. A. *Organometallics* **1999**, *18*, 2509.

Table 1. Analytical and Physical Data

compd	color	yield (%)	ν_{max}(CO)[a] (cm^{-1})	anal[b] (%) C	anal[b] (%) H
[1,6-{Cu(PPh$_3$)}-1,7-{Cu(PPh$_3$)}-6,7-(μ-H)$_2$-1,1,1-(CO)$_3$-2-Ph-*closo*-1,2-MnCB$_9$H$_7$] (**3a**)	yellow	50	2002 s, 1945 s, 1916 s	54.7 (54.3)[c]	4.6 (4.4)
[1,3-{Ni(dppe)}-3-(μ-H)-1,1,1-(CO)$_3$-2-Ph-*closo*-1,2-MnCB$_9$H$_8$] (**5a**)	burgundy	38	2029 vs, 1987 m, 1962 m	51.8 (51.9)[d]	4.7 (4.7)
[1,3,6-{Pd(dppe)}-3,6-(μ-H)$_2$-1,1,1-(CO)$_3$-2-Ph-*closo*-1,2-MnCB$_9$H$_7$] (**5b**)	indigo	59	2023 vs, 1968 w, 1934 m	51.5 (51.5)	4.7 (4.6)
[3,6-{Pt(dppe)}-3,6-(μ-H)$_2$-1,1,1-(CO)$_3$-2-Ph-*closo*-1,2-MnCB$_9$H$_7$] (**6**)	violet	63	ca. 2022 (sh) m, 2008 vs, 1949 m, 1920 m	45.7 (45.2)[c]	4.0 (4.1)
[1-Ph-2,2,2-(CO)$_3$-7-OEt-8,8-(dppe)-*hypercloso*-8,2,1-PtMnCB$_9$H$_8$] (**7a**)	green	72	2003 vs, 1938 m	47.2 (47.0)	4.5 (4.4)
[1-Ph-2,2,2-(CO)$_3$-8,8-(dppe)-*hypercloso*-8,2,1-PtMnCB$_9$H$_9$] (**7b**)	green	83	2007 vs, 1944 m	45.3 (45.2)[c]	4.4 (4.1)
[1-Ph-2,2,2-(CO)$_3$-7-OMe-8,8-(dppe)-*hypercloso*-8,2,1-PtMnCB$_9$H$_8$] (**7c**)	green	71	2005 vs, 1939 m	46.2 (46.4)	4.7 (4.2)
[1-Ph-2,2,2-(CO)$_3$-7-{O(CH$_2$)$_2$OH}-8,8-(dppe)-*hypercloso*-8,2,1-PtMnCB$_9$H$_8$] (**7d**)	green	48	2004 vs, 1940 m	46.2 (46.2)	4.3 (4.3)
[1-Ph-2,2,2-(CO)$_3$-7-{O(CH$_2$)$_4$OH}-8,8-(dppe)-*hypercloso*-8,2,1-PtMnCB$_9$H$_8$] (**7e**)	green	49	2004 vs, 1934 m	48.6 (48.5)[e]	5.3 (5.0)
[1-Ph-2,2,2-(CO)$_3$-7-{OCH$_2$C≡CH}-8,8-(dppe)-*hypercloso*-8,2,1-PtMnCB$_9$H$_8$] (**7f**)	green	28	2005 vs, 1938 m	49.2 (49.0)[e]	5.1 (4.6)
[3,6,7-{Mn(CO)$_3$}-3,7-(μ-H)$_2$-1-Ph-6,6-(dppe)-*closo*-6,1-PtCB$_8$H$_6$] (**8**)	red-orange	5	2022 vs, 1943 m	46.2 (46.4)[f]	4.0 (4.0)

[a] Measured in CH_2Cl_2; in addition, the spectra of all compounds show a broad, medium-intensity band at ca. 2500−2550 cm^{-1} due to B−H absorptions. [b] Calculated values are given in parentheses. [c] Cocrystallized with 0.5 mol equiv of CH_2Cl_2. [d] Cocrystallized with 1.5 mol equiv of CH_2Cl_2. [e] Cocrystallized with 0.5 mol equiv of C_5H_{12}. [f] Cocrystallized with 0.25 mol equiv of CH_2Cl_2.

Table 2. ^{1}H and ^{13}C NMR Data[a]

compd	^{1}H (δ[b])	^{13}C (δ[c])
1b	8.05−7.00 (br m, 35H, Ph), 3.22 [q, *J*(HH) = 7, 8H, NCH$_2$], 1.28 (t, 12H, Me)	225.5 (CO), 156.5, 135.1−126.8 (Ph), 53.0 (CH$_2$), 51.8 (br, cage C), 7.8 (Me)
3a	7.95 (m, 2H, cage Ph$_{ortho}$), 7.54−7.44 (m, 30H, PPh), 7.32 (m, 2H, cage Ph$_{meta}$), 7.22 (m, 1H, cage Ph$_{para}$)	218.4 (CO), 149.4, 136.4−126.1 (Ph), 67.5 (br, cage C)
5a	7.84 (br, 2H, cage Ph), 7.73−7.53 (br m, 20H, PPh), 7.30 (br, 3H, cage Ph), 2.27, 2.23 (m × 2, 2H × 2, CH$_2$ × 2)	223.2 (CO),[d] 149.6, 133.5−127.3 (Ph), 27.1 (br, CH$_2$)
5b	7.85 (br, 2H, cage Ph), 7.65−7.55 (br, 20H, PPh), 7.29 (br, 3H, cage Ph), 2.43 (br, 4H, CH$_2$)	221.9 (CO),[d] 149.5, 133.5−127.1 (Ph), 27.4 (br, CH$_2$)
6	7.94 (m, 2H, cage Ph$_{ortho}$), 7.73−7.55 (m, 20H, PPh), 7.34 (m, 2H, cage Ph$_{meta}$), 7.25 (m, 1H, cage Ph$_{para}$), 2.50 [d, *J*(PH) = 18, 4H, CH$_2$]	221.0 (CO),[e] 150.2, 134.2−121.1 (Ph), 114.9 (br, cage C),[f] 27.6 (br, CH$_2$)
7a	7.89 (br, 2H, cage Ph), 7.61−7.54 (m, 20H, PPh), 6.87 (m, 3H, cage Ph), 3.54, 3.05 [dq × 2, ^2J(HH) = 11, ^3J(HH) = 7, 1H × 2, OCH × 2], 2.84, 2.30 (br m × 2, 2H × 2, PCH$_2$ × 2), 0.79 (t, 3H, Me)	222.0 (CO), 147.1, 134.8−124.2 (Ph), 66.3 (OCH$_2$), 49.4 (br, cage C), 29.4, 26.8 (br × 2, PCH$_2$ × 2), 17.5 (Me)
7b	7.78 (br, 2H, cage Ph), 7.67−7.55 (m, 20H, PPh), 6.95 (m, 1H, cage Ph), 6.89 (m, 2H, cage Ph), 2.84, 2.29 (br m × 2, 2H × 2, CH$_2$ × 2)	221.3 (CO),[d] 147.3, 134.1−124.2 (Ph), 28.4 (br, CH$_2$)
7c	7.66−7.49 (m, 22H, PPh and cage Ph), 6.94 (m, 3H, cage Ph), 3.22 (s, 3H, Me), 2.76, 2.39 (br m × 2, 2H × 2, PCH$_2$ × 2)	221.7 (CO), 147.2, 134.3−124.2 (Ph), 59.0 (OMe), 50.0 (br, cage C),[f] 28.6 (CH$_2$)
7d	7.97−7.24 (br m, 22H, PPh and cage Ph),[g] 6.95 (m, 3H, cage Ph), 3.56, 3.26 (br m × 2, 1H × 2, BOCH × 2), 3.13 (m, 2H, HOC*H*$_2$), 2.99, 2.59 (br m × 2, 2H × 2, PCH$_2$ × 2)	221.4 (CO), 146.5, 134.8−124.0 (Ph), 71.6 (BOCH$_2$), 62.9 (HOCH$_2$), 48.8 (br, cage C), 28.6 (br, PCH$_2$)
7e	7.95−7.26 (br m, 22H, PPh and cage Ph),[g] 6.92 (m, 3H, cage Ph), 3.54, ca. 3.1 (br m × 2, 1H × 2, BOCH × 2), 3.04 (m, 2H, HOC*H*$_2$), 2.90, 2.45 (br m × 2, 2H × 2, PCH$_2$ × 2), 2.06 [br m, 4H, BOCH$_2$(C*H*$_2$)$_2$CH$_2$OH]	221.6 (CO), 146.9, 134.5−123.8 (Ph), 70.7 (BOCH$_2$), 62.7 (HOCH$_2$), 49.0 (br, cage C), 30.1, 29.8 (OCH$_2$*C*H$_2$CH$_2$), 28.9 (br, PCH$_2$)
7f	7.87−7.33 (br m, 22H, PPh and cage Ph), 6.95 (m, 3H, cage Ph), 4.98 (br, 1H, ≡CH), 4.13, 3.63 (m × 2, 1H × 2, OCH × 2), 2.87, 2.33 (br m × 2, 2H × 2, PCH$_2$ × 2)	221.5 (CO),[d] 146.6, 136.1−123.9 (Ph), 115.3 (C≡*C*H), 84.4 (*C*≡CH), 71.8 (OCH$_2$), 29.9, 26.8 (br × 2, PCH$_2$ × 2)
8	7.77−7.00 (m, 25H, Ph), 2.89 (br m, 2H, PCH$_2$), 2.63, 2.24 (m × 2, 1H × 2, PCH$_2$), ca. −9.3 (vbr, 2H, B−H ⇀ Mn)	208.7 (CO),[d] 139.9, 133.3−128.9 (Ph), 32.0 (br, CH$_2$)

[a] Chemical shifts (δ) in ppm; coupling constants (*J*) in hertz; measurements at ambient temperatures, except where indicated otherwise, in CD_2Cl_2. [b] Resonances for terminal BH protons occur as broad unresolved signals in the range δ from ca. −1 to +3. [c] ^{1}H-decoupled chemical shifts are positive to high frequency of SiMe$_4$. [d] The (broad) resonance for the cage carbon atom was not observed: the spectrum is weak as a result of poor solubility. [e] Recorded at 243 K. [f] Tentative assignment. [g] Resonance for terminal OH proton was not observed.

1,1,1-(CO)$_3$-2-Ph-*closo*-1,2-MnCB$_9$H$_7$] (**5b**, Chart 2). These species were characterized by the data in Tables 1−3 and by an X-ray diffraction study of **5b**. The latter afforded the structure shown in Figure 1. The molecule consists of a five-coordinate Pd(II) fragment that is bonded exo-polyhedrally to the manganacarborane surface. In addition to the two cisoid phosphorus donors, the coordination at the Pd^{II} center in **5b** is completed by a dative bond from the manganese vertex and by two three-center, two-electron B−H ⇀ Pd agostic-type interactions [Pd(1)···H(3) 2.56(4), Pd(1)···B(3) 2.257(5); Pd(1)···H(6) 2.31(4), Pd(1)···B(6) 2.356(5) Å]. As discussed previously,[4] precise electron distributions cannot definitively be assigned to the metal centers in molecules of type **5**. Different canonical forms with or without metal−metal donor bonds equally represent the electron counts at the metal centers. The two B−H ⇀ Pd bonds in **5b** involve the boron vertexes B(3) and B(6), which are in γ and β sites, respectively, relative to the carbon atom in the Mn-bound

Table 3. ^{11}B and ^{31}P NMR Data[a]

compd	^{11}B (δ[b])	^{31}P (δ[c])
3a	15.5, 7.4, 3.9, −7.9 (2B), −26.9 (2B), −28.5 (2B)	8.2 (br)
5a	28.7 (br), 15.6, 12.4, ca. 8.8 (vbr), −2.6 (br, 2B), −12.2 (3B)	58.4
5b	25.3 (br, 3B), 7.9 (br), −5.0 (vbr, 3B),−11.4 (2B)	63.1
6	16.1, 8.6, 4.7 (3B), −10.2 (2B), −16.0 (2B)	57.4 (3290)
7a	56.7, 22.6, ca. 15.8 (sh), 13.3 (2B), 2.9, −4.5 (2B), −20.3	54.4 (2570), 52.4 (2610)
7b	59.2, 22.8, 15.1 (2B), 11.1, 7.1, −1.2, −4.0, −20.7	55.9 (2580)
7c	58.3, 22.6, 14.3 (2B), ca. 12.2 (sh), 4.3, −3.9 (2B), −20.6	55.0 (2520), 52.7 (2650)
7d	56.7, 22.5, ca. 16.6 (sh), 14.0 (2B), 2.1, −4.4 (2B), −20.2	53.7 (2620), 52.8 (2590)
7e	57.2, 22.6, 13.7 (br, 3B), 2.8, −4.4 (2B), −20.3	53.8 (2560), 51.9 (2620)
7f	58.4, 22.9, ca. 15.5 (sh), 13.8 (2B), 2.7, −4.4 (2B), −20.2	54.3 (2520), 52.9 (2660)
8	50.2, 4.5 (br), ca. −3.6 (sh), −4.2, −7.7, −12.8, −19.4, −21.4	34.3 (2960), 33.6 (2780)

[a] Chemical shifts (δ) in ppm; measurements at ambient temperatures in CD_2Cl_2. [b] ^1H-decoupled chemical shifts are positive to high frequency of $BF_3{\cdot}Et_2O$ (external); resonances are of unit integral except where indicated otherwise; and where peaks are broad, the assigned integrals are somewhat subjective. [c] ^1H-decoupled chemical shifts are positive to high frequency of 85% H_3PO_4 (external). Numbers in parentheses are ^1J(PtP) coupling constants (Hz). The spectra for compounds **6**−**8** are all rather broad and suffer from low sample concentration as a result of poor solubility: quoted coupling constants are, therefore, somewhat approximate, and ^2J(PP) couplings could not be resolved.

Chart 2

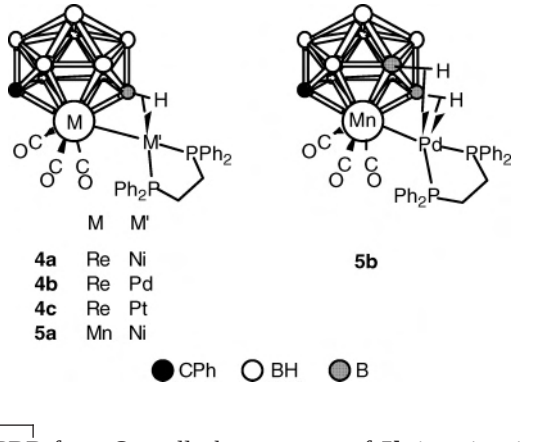

CB*BB*BB face. Overall, the structure of **5b** is quite similar to that found in **4c**, save that the agostic-type bridges in **5b** are approximately equivalent, whereas in **4c**, the B−H ⇀ Pt interaction involving the γ-BH is much stronger than that involving the β-BH. Although the Pd···B distances here are similar to those seen previously in comparable species [2.333(4)−2.406(4) Å],[11,12] the Pd···H distances determined for **5b** are much longer than those in the same compounds (ca. 1.74−1.95 Å). In effect, the {Pd(1)P(1)P(2)} plane in **5b** is twisted so that it lies between those through {Mn(1)-Pd(1)B(3)} and {Mn(1)Pd(1)B(6)} and this effectively lengthens the observed Pd···H distances. A vector to Pd(1) from a position that is an average of the two B−H ⇀ Pd bridges would complete a more genuinely square-planar coordination sphere around the palladium center. The observed "twisting", however, likely occurs in order most effectively to satisfy a five-coordinate geometry; it might also be affected by crystal packing.

The presence in **5b** of a Mn−Pd bond [Mn(1)−Pd(1) is 2.6627(7) Å] is noteworthy as relatively few examples of such exist in the literature[13] and, of those reported and

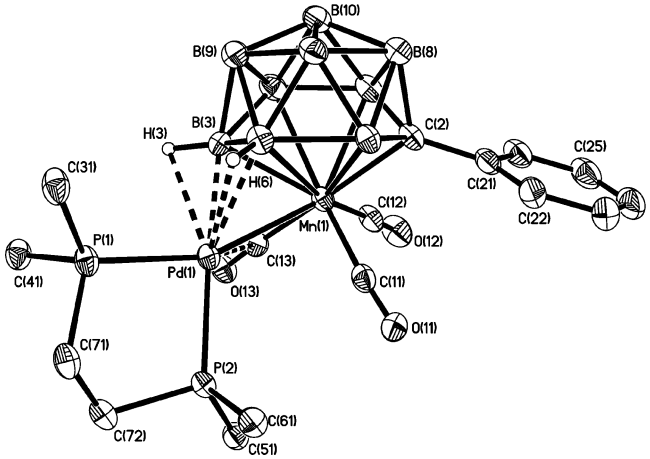

Figure 1. Structure of **5b** showing the crystallographic labeling scheme. In this and the subsequent figures, thermal ellipsoids are drawn at the 40% probability level, and for clarity, only the ipso carbon atom of the phosphine phenyl rings and only chemical significant H atoms are shown. Selected internuclear distances (Å) and angles (deg): Mn(1)−Pd(1) 2.6629(7), Mn(1)−C(2) 2.078(4), Mn(1)−B(3) 2.205(5), Mn(1)−B(4) 2.312(5), Mn(1)−B(5) 2.362(5), Mn(1)−B(6) 2.466(5), Mn(1)−B(7) 2.386(5), B(3)···Pd(1) 2.257(5), Pd(1)···H(3) 2.56(4), B(6)···Pd(1) 2.356(5), Pd(1)···H(6) 2.31(4), C(13)···Pd(1) 2.450(4); B(3)−Pd(1)−P(1) 104.75(12), B(3)−Pd(1)−P(2) 163.78(14), P(1)−Pd(1)−B(6) 105.20(12), P(2)−Pd(1)−B(6) 147.73(13), P(1)−Pd(1)−Mn(1) 157.15(3), P(2)−Pd(1)−Mn(1) 118.46(3).

structurally characterized, the metal−metal bond is generally constrained by a bridging ligand. In compound **5b**, the carborane moiety could also be considered to bridge the Mn−Pd connectivity, although it arguably does so less restrictively than units such as $Ph_2PCH_2PPh_2$ or μ-PPh_2 in previously reported examples.[13] These considerations notwithstanding, the Mn−Pd distance in **5b** is within the range of those observed previously (ca. 2.58−2.85 Å).[13] There is also one additional, longer interaction involving the palladium atom: this is to the carbon atom of a Mn-bound CO group [Pd(1)···C(13) is 2.450(4) Å]. As a result of the latter, the Mn(1)−C(13)−O(13) angle [169.3(4)°] is slightly distorted from linearity. A similar feature is seen in the crystal structure of **4c**.[4]

(11) Blandford, I.; Jeffery, J. C.; Jelliss, P. A.; Stone, F. G. A. *Organometallics* **1998**, *17*, 1402.
(12) Lassahn, P.-G.; Lozan, V.; Wu, B.; Weller, A. S.; Janiak, C. *Dalton Trans.* **2003**, 4437.
(13) Hoskins, B. F.; Steen, R. J.; Turney, T. W. *J. Chem. Soc., Dalton Trans.* **1984**, 1831. Braunstein, P.; de Jesus, E.; Tiripicchio, A. *J. Organomet. Chem.* **1989**, *368*, C5. Braunstein, P.; Oswald, B.; Tiripicchio, A.; Camellini, M. T. *Angew. Chem., Int. Ed. Engl.* **1990**, *29*, 1140. Brunet, L.; Mercier, F.; Ricard, L.; Mathey, F. *Angew. Chem., Int. Ed. Engl.* **1994**, *33*, 742. Braunstein, P.; de Meric de Bellefon, C.; Ries, M.; Fischer, J. *Organometallics* **1998**, *7*, 332. Liu, Y.; Lee, K. H.; Vittal, J. J.; Hor, T. S. A. *J. Chem. Soc., Dalton Trans.* **2002**, 2747. Adams, R. D.; Kwon, O.-S. *J. Cluster Sci.* **2003**, *14*, 367.

Scheme 1. Formation of Compounds **7** and **8** from Compound **6**

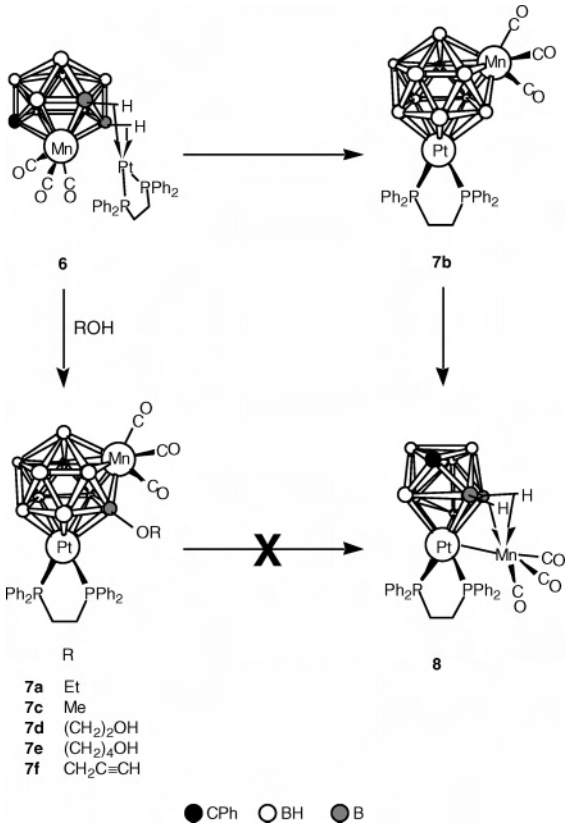

The spectroscopic data for complexes **5a** and **5b** presented in Tables 1−3 reveal some similarities but some contrasts between the two species, as well as only limited parallels with compounds **4**.[4] For example, all of compounds **4** and **5** have comparable IR spectra—albeit with some differences in the band intensities for **5a**. However, although **5a** has ^{11}B NMR parameters very similar to those for compounds **4**, those for **5b** are very different. On the basis of the former observation, the nickel species is reasonably assumed to have a structure comparable to that of complexes **4**. The X-ray diffraction study discussed above has already revealed a somewhat different geometry for **5b**; in solution, of course, both structural types might be present (possibly along with others), and the observed spectra would be the time-averaged result. Notably, both compounds **5** show only a single ^{31}P-{^{1}H} resonance at ambient temperatures. This would not be expected on the basis of the solid-state structure alone and indicates that the exo-polyhedral fragment undergoes exchange behavior that renders the two phosphorus atom environments equivalent on the NMR time scale. (Unfortunately, the poor solubilities of these complexes precluded a low-temperature study.) One such mechanism for dynamic behavior was earlier proposed for compounds **4**.[4] However, as in the Re system, the pattern of intensities in the ^{11}B{^{1}H} NMR spectra of **5a** shows the cluster to retain overall asymmetry during the fluxional process, and thus, the {M′P$_2$} fragment remains always on the same side of the notional mirror plane of the {MnCB$_9$} core. Indeed, the observed close approach of the exo-{Pd(dppe)} moiety to both BH(3) and BH(6) in **5b** in the solid state tends to lend support to the suggested[4] involvement of both of these vertexes in the migration of the exo-polyhedral fragment. Unfortunately, the broadness of the peaks in the ^{11}B{^{1}H} NMR spectrum for **5b** precludes the drawing of many conclusions about this species.

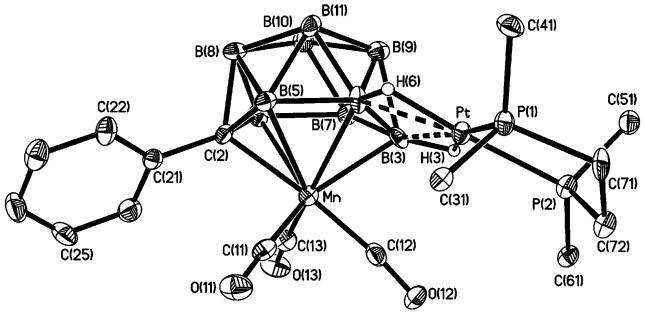

Figure 2. Structure of **6** showing the crystallographic labeling scheme. Selected internuclear distances (Å) and angles (deg): Mn−C(2) 2.083(6), Mn−B(3) 2.151(7), Mn−B(4) 2.314(8), Mn−B(5) 2.403(7), Mn−B(6) 2.379(8), Mn−B(7) 2.342(8), B(3)···Pt 2.365(7), Pt···H(3) 2.27(7), B(6)···Pt 2.205(7), Pt−H(6) 1.63(4); P(1)−Pt−B(3) 167.2(2), P(2)−Pt−B(3) 107.8(2), B(6)−Pt−P(1) 124.9(2), B(6)−Pt−P(2) 150.6(2).

Initial attempts to prepare a platinum analogue of compounds **5** via a similar synthetic route were, surprisingly, complicated by the presence in the product mixture of up to four different species. Moreover, all four of these species were confirmed spectroscopically to contain the component platinum, manganese, and carborane moieties. The picture was further confused by the observation of interconversion of these compounds. Thus, the presumed "expected" product, an initially formed dark violet species, over time gave two different green compounds and thence to a final red-orange product. Spectroscopic data alone could not unravel the details of this sequence (summarized in Scheme 1); the results from crystal structure determinations were essential in understanding this system.

Reaction between **1b**, [PtCl$_2$(dppe)], and Tl[PF$_6$] (1:1:2 ratio) gives, within ca. 15 min, a violet compound whose identity was confirmed as [3,6-{Pt(dppe)}-3,6-(μ-H)$_2$-1,1,1-(CO)$_3$-2-Ph-*closo*-1,2-MnCB$_9$H$_7$] (**6**) by an X-ray diffraction study. The structure of **6** is shown in Figure 2, and the most notable feature is the absence of a Mn−Pt bond (Mn···Pt > 3.6 Å). Instead, the exo-polyhedral {Pt(dppe)} unit is anchored to the cluster surface solely by two B−H ⇀ Pt agostic-type interactions. These involve the vertexes B(3) and B(6) that are in γ and β sites, respectively, in the manganese-bound CB*BB*BB ring, with distances [B(3)···Pt 2.365(7), Pt···H(3) 2.27(7); B(6)···Pt 2.205(7), Pt−H(6) 1.63(4) Å] that compare well with those of the sole B−H ⇀ Pt unit in **4c** [B(3)···Pt 2.266(11), Pt···H(3) 2.04-(11) Å].[4]

By itself, the geometry of **6** is relatively unremarkable, as there are multiple examples of exo-polyhedral fragments anchored to metallacarboranes without metal−metal bonds being formed.[14] However, in the present context, the structure

(14) For example: Hodson, B. E.; McGrath, T. D.; Stone. F. G. A. *Dalton Trans.* **2004**, 2570. Hodson, B. E.; McGrath, T. D.; Stone. F. G. A. *Organometallics* **2005**, *24*, 1638−1646. See also refs 3b and 8c and other references therein.

of compound **6** does contrast with those determined for **4c** and **5b** and, hence, with all five of the analogous compounds **4** and **5**. The changes observed in the sequence {**4** and **5a**} → **5b** → **6** can be viewed as a smooth progression from compounds with strong metal−metal bonding and only a single B−H ⇀ M′ bond through to a compound with only B−H ⇀ Pt bonds. This absence of a direct Mn−Pt bond is very likely a consequence of an energy and size "mismatch" between manganese- and platinum-based orbitals.

The NMR spectroscopic properties of compound **6** (Tables 2 and 3) also reveal some variation from compounds **4** and **5**. In particular, the $^{11}B\{^1H\}$ NMR parameters for **6** are noticeably different from those of its ostensible analogues **4** and **5a**. Indeed, the 1:1:3 (1 + 2 coincidence):2:2 intensity pattern in this spectrum is suggestive of overall molecular mirror symmetry on the NMR time scale, a feature that is absent from the data for compounds **4** and **5a**. The observation of only a single resonance (with ^{195}Pt satellites) in the $^{31}P\{^1H\}$ NMR spectrum of **6** and only a single broad ^1H NMR signal for the phosphine methylene groups indicates that the exo-polyhedral fragment is fluxional with respect to the cluster surface. Combined with the ^{11}B data, this tends to suggest an exchange process in which the platinum fragment migrates across the mirror plane of the $\{MnCB_9\}$ core. The extremes of such a process might involve, for example, the two enantiomers observed in the solid state, but whether any intermediate has a Mn−Pt bond can only be speculated at this stage. It is notable, however, that pure samples of compound **6**, upon dissolution, give an infrared spectrum (Table 1) whose CO stretching region clearly shows *four* bands, indicating the presence of more than one distinguishable species on the IR time scale. On the basis of this information alone, of course, it is impossible to obtain definitive identities. However, there is the tantalizing suggestion of a metal−metal bonded species similar to the Ni and Pd derivatives, with the highest-frequency CO stretch (ca. 2022 cm^{-1}, shoulder) corresponding closely to that [2029 (**5a**), 2023 (**5b**) cm^{-1}] in compounds **5**.

The second product identified in the original synthesis of **6** was the closed, 12-vertex species [1-Ph-2,2,2-$(CO)_3$-7-OEt-8,8-(dppe)-*hypercloso*-8,2,1-$PtMnCB_9H_8$] (**7a**), identified as such by a preliminary X-ray diffraction structural study. In this compound, the formerly exo-polyhedral platinum center has inserted into the 11-vertex {*closo*-1,2-$MnCB_9$} cluster of the precursor to give a species with pseudo-icosahedral {8,2,1-$PtMnCB_9$} architecture. In addition, one boron vertex [B(7)] bears an ethoxy substituent. The origin of the latter group was identified as traces of residual EtOH from the workup of the starting material **1b**. When **1b** was scrupulously freed of EtOH by recrystallization from acetone/petroleum ether, no **7a** was observed, and under these conditions, compound **6** was obtained in superior yields and as essentially the only product after a reaction time of ca. 30 min. Conversely, deliberate addition of EtOH to solutions of **6**—or to an otherwise "alcohol-free" mixture of **1b**, [$PtCl_2$-(dppe)], and Tl[PF_6]—readily afforded compound **7a**.

Although yields of **6** could be improved by elimination of EtOH and of the side formation of compound **7a**, even under these circumstances, a second green species always accompanied **6** in small amounts. Moreover, solutions of **6** also became green after several hours. In each case, the complex formed was the same and corresponds to the second green product that was obtained in trace amounts during the original attempts to prepare compound **6**, as discussed above. This product is [1-Ph-2,2,2-$(CO)_3$-8,8-(dppe)-*hypercloso*-8,2,1-$PtMnCB_9H_9$] (**7b**); it is, in fact, an isomer of **6** and is the non-*B*-substituted analogue of **7a**. Its structure was likewise confirmed by a preliminary X-ray diffraction study and by comparison of its NMR data with those of **7a** (see below).

It was of interest to establish whether other alcohols could be used as substrates to form analogues of compound **7a**. In so doing, it was hoped that some additional functionality could be appended via the boron vertexes of the $\{PtMnCB_9\}$ cluster: the introduction of substituents to (hetero)boranes is an area of considerable current interest.[3b,9,15] Thus, treatment of CH_2Cl_2 solutions of **6** with various alcohols ROH gave the *B*-substituted products [1-Ph-2,2,2-$(CO)_3$-7-OR-8,8-(dppe)-*hypercloso*-8,2,1-$PtMnCB_9H_8$] [R = Me (**7c**), $(CH_2)_2OH$ (**7d**), $(CH_2)_4OH$ (**7e**), $CH_2C{\equiv}CH$ (**7f**)]. It had been hoped that using diols in this reaction would afford linked bis(cage) species, but this proved not to be the case. Nevertheless, the additional terminal functionality that remains on the substituents in compounds **7d**−**7f** bodes well for future reactivity studies that might exploit these features. Attempts were also made to employ in this reaction other substrates containing a potentially protonic H atom that could combine with a boron-bound hydride and eliminate as H_2, but these proved unsuccessful. With secondary amines, for example, the exo-polyhedral platinum fragment was simply abstracted by the N donor: spectroscopic analysis of the product mixture showed the anion of **1b** as the only metallacarborane product. It should also be noted at this juncture that compounds **5** appear to be relatively stable in the presence of traces of EtOH but decompose with excess of the alcohol: analysis of the details of these reactions are continuing.

An X-ray diffraction study of compound **7d** revealed the structure shown in Figure 3. The preliminary structural determinations for compounds **7a** and **7b** mentioned earlier showed identical connectivity patterns, with the only differences being the substituent bound to B(7). In **7d**, specifically, this substituent is an $-OCH_2CH_2OH$ unit, with B(7)−O(71) being 1.392(5) Å. Perhaps surprisingly, the hydrogen atom of the pendant OH group in **7d** does not hydrogen bond with the OH of an adjacent molecule. Instead, this hydrogen atom appears oriented so that it points toward the center of one of the phosphine phenyl rings, forming an intramolecular

(15) Other recent examples include: Robertson, S.; Ellis, D.; McGrath, T. D.; Rosair, G. M.; Welch, A. J. *Polyhedron* **2002**, *22*, 1293. Yao, H.; Grimes, R. N.; Corsini, M.; Zanello, P. *Organometallics* **2003**, *22*, 4381. Rojo, I.; Teixidor, F.; Viñas, C.; Kivekäs, R.; Sillanpää, R. *Chem. Eur. J.* **2003**, *9*, 4311. Olejniczak, A. B.; Plesek, J.; Kriz, O.; Lesnikowski, Z. J. *Angew. Chem., Int. Ed.* **2003**, *42*, 5740. Hawthorne, M. F. *Pure Appl. Chem.* **2003**, *75*, 1157. Franken, A.; Carr, M. J.; Clegg, W.; Kilner, C. A.; Kennedy, J. D. *Dalton Trans.* **2004**, 3552. See also: Grimes, R. N. *Coord. Chem. Rev.* **2000**, *200*−*202*, 773. Davidson, M. G., Hughes, A. K., Marder, T. B., Wade, K., Eds.; *Contemporary Boron Chemistry*; Royal Society of Chemistry: Cambridge, U.K., 2000.

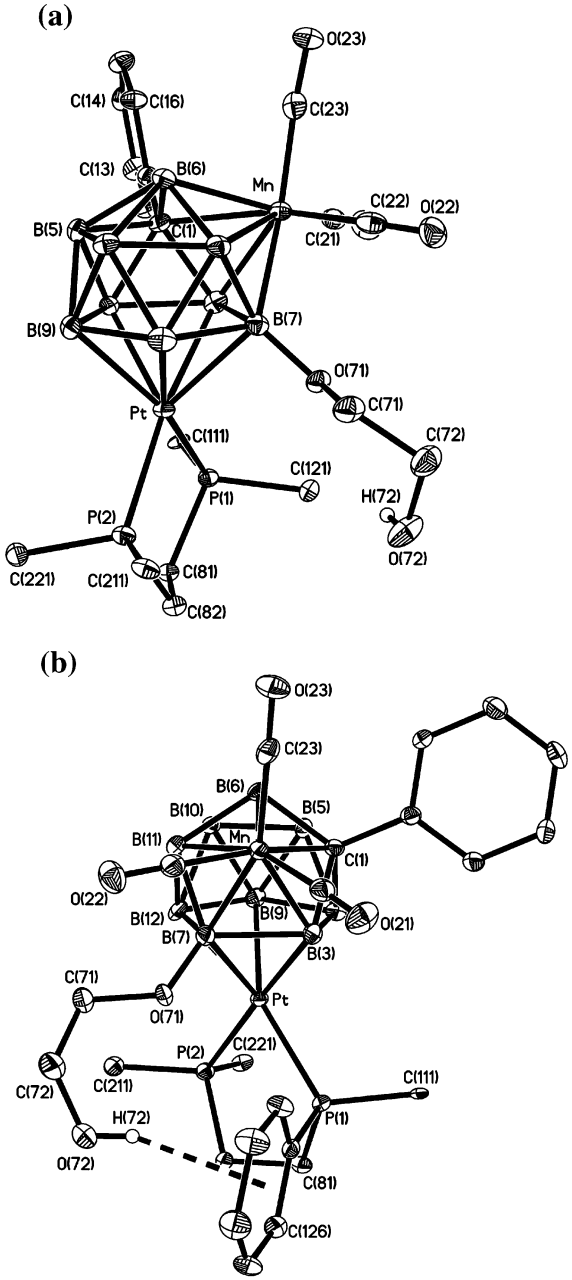

Figure 3. Two views of the structure of **7d** showing the crystallographic labeling scheme: (a) general perspective and (b) view, including the relevant P−Ph ring, that emphasizes the O−H···π hydrogen bond. Selected internuclear distances (Å) and angles (deg): Mn−C(1) 2.203(4), Mn−B(3) 2.130(5), Mn−B(6) 2.173(5), Mn−B(7) 2.136(5), Mn−B(11) 2.265(5), B(3)−Pt 2.258(5), B(4)−Pt 2.191(4), B(7)−O(71) 1.392(5), B(7)−Pt 2.265(5), B(9)−Pt 2.263(5), B(12)−Pt 2.268(5); O(71)−B(7)−Mn 121.8(3), O(71)−B(7)−Pt 96.5(3), B(7)−Pt−P(2) 127.25(12), B(7)−Pt−P(1) 113.85(13). The H(72)···X distance is ca. 2.57 Å, the O(71)···X distance is ca. 3.35 Å, and the O−H···X angle is ca. 156°; X is the C(12*n*) (n = 1−6) ring centroid.

O−H···π hydrogen bond (Figure 3b).[16] The H···X (X = ring centroid) distance is ca. 2.57 Å, while O(71)···X is ca. 3.35 Å and the O−H···X angle is ca. 156 °, typical values for such interactions in organometallic species.[16c]

Apart from this feature, the structure is at first sight relatively unremarkable, and the geometry of the cluster in compounds **7** is confirmed as a closed 12-vertex {8,2,1-PtMnCB$_9$} pseudo-icosahedron. In this structure, the manganese center is coordinated on one side by three CO ligands and on the other side by the $\overline{\text{CBBBB}}$ face of a {*nido*-4,7-PtCB$_9$} cage; the alkoxide-substituted boron vertex is in a β position with respect to the carbon atom within this face. This β site is well established as the one favored for substitution in the related compounds where the $\overline{\text{CB}\textit{B}\text{BB}}$ face of a {*nido*-7-CB$_{10}$} ligand is bonded to a metal center.[3b] Around the platinum vertex, the coordination sphere comprises the two phosphorus donors of the dppe ligand, plus the five boron atoms in the η^5-B$_5$ face of a {*nido*-3,2-MnCB$_9$} unit. The latter coordination, with the cage carbon atom in the "upper" belt of the ligand, resembles the platinum-to-carborane bonding in a Pt^{IV} polytellurium species where a {Pt(PEt$_3$)L$_2$} unit [L$_2$ = Te(Ph)−Pt(TePh)PEt$_3$−Te(Ph)] is coordinated by the η^5-B$_5$ face of a {*nido*-2-CB$_{10}$} carborane.[17] Isolobal replacement of {Mn(CO)$_3$} ↔ {BH}$^+$ vertexes would relate the two platinum-bound subclusters. The substituted boron atom B(7) is adjacent also to the platinum center in **7d**, and of the two boron atoms bonded to both metal vertexes, this one is the more distant from the cage carbon; hence, substitution here is readily understood in terms of this being the most hydridic {BH} in the parent (that is, in **7b**).

The cluster architecture of compounds **7** presents an interesting conundrum in electron-counting terms. If the {PtP$_2$}^{0} unit is considered to be a two-electron donor for cluster bonding, as is usual,[18] then insertion of a {PtP$_2$}$^{2+}$ unit into the conventionally closo 11-vertex {MnCB$_9$} cluster (with 24 skeletal electrons, i.e., $2n + 2$ cluster bonding pairs,[19] where n is the number of cluster vertexes) would not increase the cluster electron count. Thus, the {PtMnCB$_9$} cluster of **7** would then be described as hypercloso,[20] having $2n$ skeletal bonding pairs. However, the connectivity pattern in compounds **7** resembles that of a conventional closo-structured icosahedron, rather than that normally found in hypercloso 12-vertex species.[21] This observation might imply that the {PtP$_2$} unit behaves here as a four-electron contributor, as a result of the platinum center tending toward a 16-electron configuration and donating an additional electron pair from a lower lying, filled orbital.[18,22]

(16) (a) Viswamitra, M. A.; Radhakrishnan, R.; Bandekar, J.; Deriaju, G. R. *J. Am. Chem. Soc.* **1993**, *115*, 4868. (b) Malone, J. F.; Murray, C. M.; Charlton, M. H.; Docherty, R.; Lavery, A. J. *J. Chem. Soc., Faraday Trans.* **1997**, *93*, 3429. (c) Braga, D.; Grepioni, F.; Tedesco, E. *Organometallics* **1998**, *17*, 2669.

(17) Batten, S. A.; Jeffrey, J. C.; Rees, L. H.; Rudd, M. D.; Stone, F. G. A. *J. Chem. Soc., Dalton Trans*. **1998**, 2839.

(18) O'Neill, M. E.; Wade, K. In *Comprehensive Organometallic Chemistry*; Wilkinson, G., Abel, E. W., Stone, F. G. A., Eds.; Pergamon Press: Oxford, U.K., 1982; Vol. 1, Section 1.

(19) (a) Wade, K. *Adv. Inorg. Chem. Radiochem.* **1976**, *18*, 1. (b) Mingos, D. M. P. *Acc. Chem. Res.* **1984**, *17*, 311.

(20) Baker, R. T. *Inorg. Chem.* **1986**, *25*, 109. Johnston, R. L.; Mingos, D. M. P. *Inorg. Chem.* **1986**, *25*, 3321; Johnston, R. L.; Mingos, D. M. P.; Sherwood, P. *New J. Chem.* **1991**, *15*, 831.

(21) Attfield, M. J.; Howard, J. A. K.; Jelfs, A. N. de M.; Nunn, C. M.; Stone, F. G. A. *J. Chem. Soc., Dalton Trans.* **1987**, 2219. Carr, N.; Mullica, D. F.; Sappenfield, E. L.; Stone, F. G. A. *Organometallics* **1992**, *11*, 3697.

(22) See, for example: Kennedy, J. D. In *The Borane, Carborane, Carbocation Continuum*; Casanova, J., Ed.; Wiley: New York, 1998; p 85 and references therein.

Chart 3

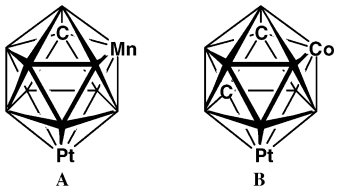

The mechanism of formation of compounds **7** at this time remains unclear. It is well-known[23] that $\{PtL_2\}^0$ units can oxidatively insert into closo carboranes, but in those cases, a zerovalent (d^{10}) platinum center is involved, and this would require a very significant electron redistribution in **6**. Moreover, such reactions of the closo 11-vertex carboranes 2,3-Me_2-*closo*-2,3-$C_2B_9H_9$, [*closo*-2-$CB_{10}H_{11}]^-$ and 2-NMe_3-*closo*-2-$CB_{10}H_{10}$ give products where the platinum and carbon vertexes remain mutually adjacent.[24,25] This is not the case in compounds **7**, but in any event, it could be argued, for example, that a sterically induced cluster rearrangement[26] occurs after insertion or, indeed, that these oxidative insertion reactions might proceed differently with metallacarborane substrates. The latter suggestion might gain support from earlier observations of the reaction of the $\{Pt(PEt_3)_2\}^0$ fragment with [1-(η-C_5H_5)-*closo*-1,2,4-$CoC_2B_8H_{10}$].[24] The product of that reaction, identified as [4-(η-C_5H_5)-7,7-$(PEt_3)_2$-*closo*-7,4,1,2-$PtCoC_2B_8H_{10}$], can be compared with compounds **7** (cluster structures **A** and **B**, respectively, in Chart 3), and it is encouraging to note considerable similarities between the arrangement of the vertexes in the two clusters.

All compounds **7** are dark green and show the expected close mutual similarities in their spectral data (Tables 1−3). Their $^{31}P\{^1H\}$ spectra all show two signals, each with ^{195}Pt satellites, indicating restricted rotation of the $\{PtP_2\}$ unit with respect to the ligating CBBBB face of the manganacarborane. For **7b**, the two ^{31}P resonances are accidentally coincident, reflecting the greater symmetry of the unsubstituted manganacarborane face. In addition to ^1H and $^{13}C\{^1H\}$ NMR resonances for the cage Ph and metal-bound dppe and CO ligands, all of the boron-bound OR groups give rise to signals in expected positions and display no unusual perturbations upon attachment to the metallacarborane. The cage carbon atom (where discernible) resonates at around δ 50 in the $^{13}C\{^1H\}$ NMR spectra of all of compounds **7**, a typical position for such a vertex. In their $^{11}B\{^1H\}$ NMR spectra, compounds **7** show nine separate resonances (with some coincidences), as required by the lack of cluster symmetry. These occur in the region δ from ca. 60 to −20, a relatively broad range for a closo carbametallaborane, and might be indicative of some loss of cluster electron density, consistent with a hypercloso descriptor[20,27] as discussed above. Unfortunately, the $^{11}B\{^1H\}$ NMR signals for these compounds are all generally rather broad, and so upon retention of proton coupling, most resonances showed only further broadening and no doublet structure could be revealed. It was, therefore, impossible to establish with certainty the chemical shift of the substituted boron atom.

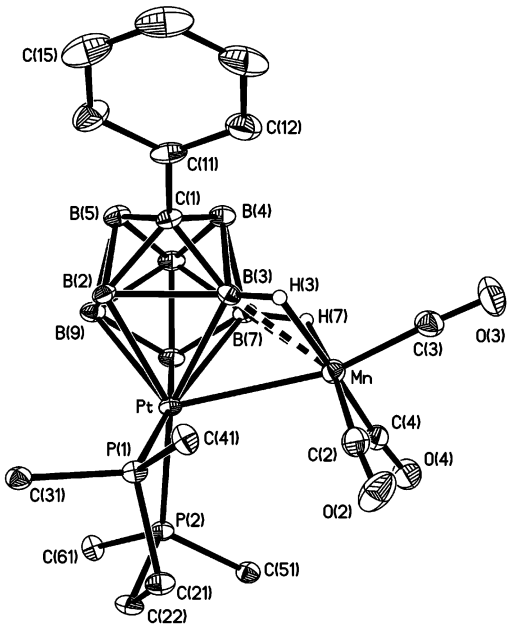

Figure 4. Structure of **8** showing the crystallographic labeling scheme. Selected internuclear distances (Å) and angles (deg): Pt−Mn 2.8088(9), Pt−B(2) 2.271(6), Pt−B(3) 2.212(6), Pt−B(7) 2.317(6), Pt−B(9) 2.395(6), Pt−B(10) 2.127(6), Mn···B(3) 2.220(6), Mn−H(3) 1.90(6), Mn···B(7) 2.181(6), Mn−H(7) 1.80(6); C(2)−Mn−Pt 93.8(2), C(3)−Mn−Pt 164.2(2), C(4)−Mn−Pt 105.43(19), B(3)−Mn−Pt 50.56(16), B(7)−Mn−Pt 53.57(16), P(1)−Pt−Mn 104.26(4), P(2)−Pt−Mn 106.84(4).

Each of compounds **7** is unstable, and **7b** is particularly so. Whereas **7a** and **7c**−**7f** apparently decompose slowly but entirely and give no identifiable metallacarborane products, **7b** upon decomposition gives small amounts of the red-orange species that was the fourth product—compound **8**—isolated in the original attempted synthesis of compound **6**. Indeed, traces of compound **8** are generally also observed during the deliberate synthesis of the other compounds **7** from **6**, this being presumably via **7b**, which must always be competitively (but relatively much more slowly) formed alongside **7a** and **7c**−**7f**. It is notable in this connection that compound **7b** cannot be purified by column chromatography, as this significantly accelerates its conversion to compound **8**. It is apparent that other metallacarboranes might also be formed in the latter process—including, for example, a possible nine-boron analogue of compound **8**—but these seem generally to be somewhat transient and unstable and are formed only in very low and variable yields.

Initial spectroscopic data, as noted earlier, confirmed the presence of platinum, manganese, and carborane moieties in compound **8**, but their precise arrangement and constitution was established only following a single-crystal X-ray diffraction experiment, whose results are depicted in Figure 4.

(23) Stone, F. G. A. *J. Organomet. Chem.* **1977**, *100*, 257.
(24) Green, M.; Spencer, J. L.; Stone, F. G. A.; Welch, A. J. *J. Chem. Soc., Dalton Trans.* **1975**, 179.
(25) Carroll, W. E.; Green, M.; Stone, F. G. A.; Welch, A. J. *J. Chem. Soc., Dalton Trans.* **1975**, 2263.
(26) For example: Baghurst, D. R.; Copley, R. C. B.; Fleischer, H.; Mingos, D. M. P.; Kyd, G. O.; Yellowlees, L. J.; Welch, A. J.; Spalding, T. R.; O'Connell, D. *J. Organomet. Chem.* **1993**, *447*, C14.
(27) Jung, C. W.; Baker, R. T.; Hawthorne, M. F. *J. Am. Chem. Soc.* **1981**, *103*, 810. Littger, R.; Englich, U.; Ruhlandt-Senge, K.; Spencer, J. T. *Angew. Chem., Int. Ed.* **2000**, *39*, 1472.

The molecule is identified as [3,6,7-{Mn(CO)$_3$}-3,7-(μ-H)$_2$-1-Ph-6,6-(dppe)-*closo*-6,1-PtCB$_8$H$_6$] and consists of a central {*closo*-6,1-PtCB$_8$} core to which is bonded an exo-polyhedral {Mn(CO)$_3$} moiety. In addition to this extrusion of the manganese vertex from the precursor **7b**, a {BH} vertex has also been lost. Within the {PtCB$_8$} unit, the carbon atom adopts the four-coordinate site, while the metal center is five-coordinate, as would be expected. These two vertexes are mutually nonadjacent, a feature preserved from the precursor **7b**. Only one other simple metallacarborane with this atom arrangement has hitherto been structurally characterized, namely, the iridacarborane [6-H-6,6,10-(PPh$_3$)$_3$-*closo*-6,1-IrCB$_8$H$_8$],[28] although that compound was prepared directly from the eight-boron carborane [*arachno*-4-CB$_8$H$_{13}$]$^-$. In addition, each of the {MoCB$_8$} subclusters in the recently reported "macropolyhedral" anion [(CO)$_2$MoB$_{16}$H$_{15}$C$_2$Ph$_2$]$^-$ has the same relative disposition of metal and carbon vertexes; this, too, was prepared from an eight-boron precursor, namely, 1-Ph-*nido*-1-CB$_8$H$_{11}$.[29]

The exo-polyhedral {Mn(CO)$_3$} unit in **8** is attached to the platinacarborane surface via a Pt−Mn bond [Pt−Mn = 2.8088(9) Å] and by two B−H ⇀ Mn agostic-type interactions involving two adjacent boron atoms [Mn···B(3) = 2.220(6), Mn−H(3) = 1.90(6); Mn···B(7) = 2.181(6), Mn−H(7) = 1.80(6) Å]. This provides a distinct contrast with compound **6**, from which a Pt−Mn bond is absent. We are aware of only one other report of a metallaheteroborane bearing an exo-polyhedral {Mn(CO)$_3$} group, namely, a monoanionic derivative obtained from compound **1a**.[4] A pair of {Mn(CO)$_4$} derivatives of {*closo*-3,1,2-RhC$_2$B$_9$} clusters are also known.[30] None of these, unfortunately, has been structurally characterized.

Spectroscopic and other physical data characterizing compound **8** are presented in Tables 1−3. In its ^{11}B{^{1}H} NMR spectrum, eight resonances of unit integral are seen, consistent with the absence of any symmetry in the solid-state structure. Likewise, the ^{31}P{^{1}H} NMR spectrum shows two separate resonances, each with ^{195}Pt satellites, also consistent with an asymmetric system. The ^{1}H and ^{13}C{^{1}H} NMR spectra exhibit signals in the appropriate positions for the cage, phosphine and carbonyl ligands, of which the most significant features are the lowering in chemical shifts of the ipso carbon atom of the cluster-bound phenyl unit and of the carbonyl groups. Of these, the former resonates at δ 139.9 in **8**, compared to δ ca. 145−155 in all of compounds **1**−**7**;[4] it is unfortunate that the signal for the cage carbon atom could not definitively be located as this would likely also reveal some further information about the electronic properties of the {PtCB$_8$} cluster in compound **8**. The manganese-bound CO groups give a single broad peak at δ 208.7 in the ^{13}C{^{1}H} NMR spectrum, compared to δ ca. 220−225 in compounds **1b**, **3a**, and **5**−**7**. The increased shielding can be attributed to the {Mn(CO)$_3$} center changing from a cluster vertex (bound to $\overline{\text{CBBBBB}}$ or $\overline{\text{CBBBB}}$ faces) to an exo-polyhedral site (bound to the platinum and by two B−H ⇀ Mn bridges). In the ^{1}H NMR spectrum, the protons involved in these agostic-type interactions give rise to broad resonances coincident at δ ca. −9.3, typical for such hydrogens.[4,30]

Conclusion

The reactions of the mangana(tricarbonyl)carborane salt **1b** reported herein, together with those described previously for its rhenium analogue **1a**,[4,6] have revealed that a rich chemistry is associated with subicosahedral, "half-sandwich" metal monocarbollide cage frameworks. These new results further exemplify the variety of novel compounds that can be derived from monocarbollide complexes in general,[3b] as opposed to their dicarbollide[31] analogues. Of particular interest in the present work is the unprecedented spontaneous insertion of the exo-polyhedral platinum fragment into the manganacarborane cluster in compound **6**, providing the novel dimetallacarboranes **7**. Equally intriguing is the conversion of **7b** to **8**, via extrusion of boron and manganese vertexes, which completes the series whereby manganese and platinum centers exchange exo- and endo-polyhedral sites. Although it seems clear that this exchange proceeds via a 12-vertex dimetal intermediate, the details of the mechanism and the reasons for this behavior are less clear. Our studies of these and related systems, as well as our attempts to identify other trace products in these reactions, are continuing.

Experimental Section

General Considerations. All reactions were carried out under an atmosphere of dry, oxygen-free nitrogen using standard Schlenk line techniques. Solvents were distilled from appropriate drying agents under nitrogen prior to use. Petroleum ether refers to that fraction of boiling point 40−60 °C. Chromatography columns (typically ca. 15 cm in length and ca. 2 cm in diameter) were packed with silica gel (Acros, 60−200 mesh). Celite pads used for filtration were typically ca. 3 cm in depth and 2 cm in diameter. NMR spectra were recorded at the following frequencies (MHz): ^{1}H, 360.1; ^{13}C, 90.6; ^{11}B, 115.5; ^{31}P, 145.8. The compounds [NEt$_4$][6-Ph-*nido*-6-CB$_9$H$_{11}$],[32] [Mn(NCMe)$_3$(CO)$_3$][PF$_6$],[33] and [CuCl(PPh$_3$)]$_4$[34] were prepared by literature methods; [NiCl$_2$(dppe)] was formed from NiCl$_2$ and dppe in refluxing EtOH (15 min); and the complexes [PdCl$_2$(dppe)] and [PtCl$_2$(dppe)] were obtained by addition of dppe to a CH$_2$Cl$_2$ solution of [MCl$_2$(NCPh)$_2$] (M = Pd, Pt).[35] All other reagents were used as received.

Synthesis of [N(PPh$_3$)$_2$][NEt$_4$][1,1,1-(CO)$_3$-2-Ph-*closo*-1,2-MnCB$_9$H$_9$]. A THF (20 mL) solution of [NEt$_4$][6-Ph-*nido*-6-

(28) Alcock, N. W.; Taylor, J. G.; Wallbridge, M. G. H. *J. Chem. Soc., Chem. Commun.* **1983**, 1168.
(29) Carr, M. J.; Franken, A.; Kennedy, J. D. *Dalton Trans.* **2004**, 2612.
(30) Jeffery, J. C.; Stone, F. G. A., Topaloğlu, I. *J. Organomet. Chem.* **1993**, *451*, 205.
(31) Ellis, D. D.; Jelliss, P. A.; Stone, F. G. A. *Organometallics* **1999**, *18*, 4982. Ellis, D. D.; Jelliss, P. A.; Stone, F. G. A. *J. Chem. Soc., Dalton Trans.* **2000**, 2113. Ellis, D. D.; Jeffery, J. C.; Jelliss, P. A.; Kautz, J. A.; Stone, F. G. A. *Inorg. Chem.* **2001**, *40*, 2041.
(32) Jelínek, T.; Thornton-Pett, M.; Kennedy, J. D. *Collect. Czech. Chem. Commun.* **2002**, *67*, 1035. See also: Brellochs, B. In *Contemporary Boron Chemistry*; Davidson, M. G., Hughes, A. K., Marder, T. B., Wade, K., Eds.; Royal Society of Chemistry: Cambridge, U.K., 2000; p 212.
(33) Reiman, R. H.; Singleton, E. *J. Chem. Soc., Dalton Trans.* **1974**, 808.
(34) Mann, F. G.; Purdie, D. *J. Chem. Soc.* **1935**, 1549. Jardine, F. H.; Rule, J.; Vohra, G. A. *J. Chem. Soc. A* **1970**, 238.
(35) Anderson, G. K.; Lin, M. *Inorg. Synth.* **1990**, *28*, 61.

Table 4. Crystallographic Data for **5b**·$2CH_2Cl_2$, **6**·CH_2Cl_2, **7d**·CH_2Cl_2, and **8**·$2CH_2Cl_2$[a]

	5b·$2CH_2Cl_2$[b]	**6**·CH_2Cl_2	**7d**·CH_2Cl_2	**8**·$2CH_2Cl_2$
formula	$C_{38}H_{40}B_9Cl_4MnO_3P_2Pd$	$C_{37}H_{40}B_9Cl_2MnO_3P_2Pt$	$C_{39}H_{44}B_9Cl_2MnO_5P_2Pt$	$C_{38}H_{41}B_8Cl_4MnO_3P_2Pt$
fw	1007.09	1012.85	1072.90	1085.96
a, Å	10.9749(3)	10.571(2)	10.3831(13)	10.0647(11)
b, Å	11.5671(3)	12.0680(19)	11.7188(14)	11.0280(7)
c, Å	20.1699(5)	18.590(4)	18.555(2)	20.0776(18)
α, deg	92.365(2)	103.014(17)	85.961(5)	86.511(6)
β, deg	95.300(2)	95.691(17)	78.853(5)	77.386(9)
γ, deg	114.092(2)	113.966(17)	81.942(5)	88.671(8)
V, Å^3	2318.68(10)	2062.5(7)	2191.1(5)	2170.6(3)
ρ_{calcd}, g cm^{-3}	1.442	1.631	1.626	1.662
T, K	100(2)	173(2)	110(2)	173(2)
μ(Mo Kα), mm^{-1}	8.388[c]	3.937	3.714	3.867
reflns measured	18178	7687	39671	8527
indep reflns	7871	7257	11906	7997
R_{int}	0.0471	0.0284	0.0719	0.0167
wR2(all data), R1[d]	0.1332, 0.0509	0.0996, 0.0435	0.0750, 0.0470	0.1074, 0.0412

[a] All crystals were triclinic, space group $P\bar{1}$, $Z = 2$. [b] One CH_2Cl_2 solvate was refined without H atoms; the empirical formula and the values quoted for the fw, ρ_{calcd}, and μ reflect this. [c] μ(Cu Kα). [d] wR2 = $\{\sum[w(F_o^2 - F_c^2)^2]/\sum w(F_o^2)^2\}^{1/2}$ and R1 = $\sum||F_o| - |F_c||/\sum|F_o|$, with $F_o > 4\sigma(F_o)$.

CB_9H_{11}] (0.411 g, 1.26 mmol) was cooled to −78 °C and ^{n}BuLi (1.0 mL, 2.5 M solution in hexanes, 2.50 mmol) was added. After the mixture had warmed to ca. −40 °C, $[Mn(NCMe)_3(CO)_3][PF_6]$ (0.511 g, 1.26 mmol) was added. The mixture was warmed to room temperature and was stirred at this temperature for 3 h; $[N(PPh_3)_2]Cl$ (1.40 g, 2.44 mmol) was then added, and stirring was continued overnight. A yellow solid precipitated that was isolated by filtration, washed with ice-cold EtOH (20 mL) and dried in vacuo to give $[N(PPh_3)_2][NEt_4][1,1,1\text{-}(CO)_3\text{-}2\text{-Ph-}closo\text{-}1,2\text{-}MnCB_9H_9]$ (**1b**) (0.92 g) as a dark yellow, microcrystalline solid. Residual EtOH was removed by recrystallization from acetone/petroleum ether.

Synthesis of [1,6-{Cu(PPh$_3$)}-1,7-{Cu(PPh$_3$)}-6,7-(μ-H)$_2$-1,1,1-(CO)$_3$-2-Ph-*closo*-1,2-MnCB$_9$H$_7$]. To a CH_2Cl_2 (20 mL) solution of **1b** (0.100 g, 0.10 mmol) was added $[CuCl(PPh_3)]_4$ (0.072 g, 0.05 mmol) and $Tl[PF_6]$ (0.070 g, 0.20 mmol), and the mixture was stirred overnight. After filtration (Celite), solvent was removed in vacuo, and the residue was applied to a chromatography column. Elution with CH_2Cl_2/petroleum ether (3:2) removed a yellow band, from which $[1,6\text{-}\{Cu(PPh_3)\}\text{-}1,7\text{-}\{Cu(PPh_3)\}\text{-}6,7\text{-}(\mu\text{-}H)_2\text{-}1,1,1\text{-}(CO)_3\text{-}2\text{-Ph-}closo\text{-}1,2\text{-}MnCB_9H_7]$ (**3a**) (0.049 g) was isolated as a yellow microcrystalline solid after removal of the solvent in vacuo.

Reactions of Compound 1b with [MCl$_2$(dppe)] (M = Ni, Pd, Pt) in the Presence of Tl[PF$_6$]. (i) Compound **1b** (0.200 g, 0.20 mmol), $[NiCl_2(dppe)]$ (0.106 g, 0.20 mmol), and $Tl[PF_6]$ (0.140 g, 0.40 mmol) were stirred overnight in CH_2Cl_2 (30 mL). The reaction mixture was filtered (Celite) and evaporated to dryness, and the residue was applied to a chromatography column. A wine fraction was eluted with CH_2Cl_2/petroleum ether (3:2), which, after removal of the solvent in vacuo, yielded $[1,3\text{-}\{Ni(dppe)\}\text{-}3\text{-}(\mu\text{-}H)\text{-}1,1,1\text{-}(CO)_3\text{-}2\text{-Ph-}closo\text{-}1,2\text{-}MnCB_9H_8]$ (**5a**) (0.060 g) as dark burgundy microcrystals.

(ii) Similarly, the compound $[1,3,6\text{-}\{Pd(dppe)\}\text{-}3,6\text{-}(\mu\text{-}H)_2\text{-}1,1,1\text{-}(CO)_3\text{-}2\text{-Ph-}closo\text{-}1,2\text{-}MnCB_9H_7]$ (**5b**) (0.099 g) was obtained as a microcrystalline indigo solid following the reaction between **1b** (0.200 g, 0.20 mmol), $[PdCl_2(dppe)]$ (0.115 g, 0.20 mmol) and $Tl[PF_6]$ (0.140 g, 0.40 mmol).

(iii) A mixture of **1b** (0.300 g, 0.30 mmol), $[PtCl_2(dppe)]$ (0.199 g, 0.30 mmol), and $Tl[PF_6]$ (0.210 g, 0.60 mmol) in CH_2Cl_2 (30 mL) was stirred for 30 min, filtered (Celite), and then evaporated to dryness in vacuo. Chromatography of the residue, eluting with CH_2Cl_2/petroleum ether (2:3), gave first a broad orange-yellow band, from which $[3,6,7\text{-}\{Mn(CO)_3\}\text{-}3,7\text{-}(\mu\text{-}H)_2\text{-}1\text{-Ph-}6,6\text{-(dppe)-}closo\text{-}6,1\text{-}PtCB_8H_6]$ (**8**) (0.014 g) was obtained as an orange-red powder. Further elution, using CH_2Cl_2/petroleum ether (3:2), removed a violet band, which, after evaporation in vacuo, gave $[3,6\text{-}\{Pt(dppe)\}\text{-}3,6\text{-}(\mu\text{-}H)_2\text{-}1,1,1\text{-}(CO)_3\text{-}2\text{-Ph-}closo\text{-}1,2\text{-}MnCB_9H_7]$ (**6**) (0.175 g) as dark purple microcrystals. Repeated column chromatography of compound **6** always afforded a few milligrams more of compound **8**.

Synthesis of the Compounds [1-Ph-2,2,2-(CO)$_3$-7-X-8,8-(dppe)-*hypercloso*-8,2,1-PtMnCB$_9$H$_8$] [X = OEt, H, OMe, O(CH$_2$)$_2$OH, O(CH$_2$)$_4$OH, OCH$_2$C≡CH]. (i) Compound **6** (0.020 g, 0.022 mmol) was dissolved in CH_2Cl_2 (30 mL), EtOH (0.05 mL) was added, and the mixture was stirred overnight. After removal of the solvent in vacuo, the residue was taken up in minimal CH_2Cl_2/petroleum ether (1:1) and applied to a chromatography column. Elution with CH_2Cl_2/petroleum ether (3:2) gave a single green fraction, from which $[1\text{-Ph-}2,2,2\text{-}(CO)_3\text{-}7\text{-OEt-}8,8\text{-(dppe)-}hypercloso\text{-}8,2,1\text{-}PtMnCB_9H_8]$ (**7a**) (0.015 g) was isolated as dark green microcrystals after removal of the solvent in vacuo.

(ii) Compound **6** (0.020 g, 0.022 mmol) was dissolved in CH_2Cl_2 (30 mL), and the solution was stirred overnight. Slow addition of the resulting dark green mixture to an excess (100 mL) of petroleum ether precipitated essentially pure $[1\text{-Ph-}2,2,2\text{-}(CO)_3\text{-}8,8\text{-(dppe)-}hypercloso\text{-}8,2,1\text{-}PtMnCB_9H_9]$ (**7b**) (0.017 g), isolated as a dark green powder. Attempted further purification by column chromatography resulted in significant conversion to compound **8**.

(iii) A solution of compound **6** (0.020 g, 0.022 mmol) in CH_2Cl_2/MeOH (2:1, 15 mL) was stirred overnight. Workup as above for compound **7a** gave dark green $[1\text{-Ph-}2,2,2\text{-}(CO)_3\text{-}7\text{-OMe-}8,8\text{-(dppe)-}hypercloso\text{-}8,2,1\text{-}PtMnCB_9H_8]$ (**7c**) (0.015 g).

(iv) By a similar procedure, compound **6** (0.100 g, 0.11 mmol) in CH_2Cl_2 (10 mL) treated with $HO(CH_2)_2OH$ (0.3 mL) gave dark green $[1\text{-Ph-}2,2,2\text{-}(CO)_3\text{-}7\text{-}\{O(CH_2)_2OH\}\text{-}8,8\text{-(dppe)-}hypercloso\text{-}8,2,1\text{-}PtMnCB_9H_8]$ (**7d**) (0.052 g).

(v) Likewise, treatment of a CH_2Cl_2 (10 mL) solution of compound **6** (0.100 g, 0.11 mmol) with $HO(CH_2)_4OH$ (0.3 mL) gave dark green $[1\text{-Ph-}2,2,2\text{-}(CO)_3\text{-}7\text{-}\{O(CH_2)_4OH\}\text{-}8,8\text{-(dppe)-}hypercloso\text{-}8,2,1\text{-}PtMnCB_9H_8]$ (**7e**) (0.055 g).

(vi) Similarly, compound **6** (0.100 g, 0.11 mmol) in CH_2Cl_2 (10 mL) with $HC{\equiv}CCH_2OH$ (0.3 mL) gave dark green $[1\text{-Ph-}2,2,2\text{-}(CO)_3\text{-}7\text{-}\{OCH_2C{\equiv}CH\}\text{-}8,8\text{-(dppe)-}hypercloso\text{-}8,2,1\text{-}PtMnCB_9H_8]$ (**7f**) (0.030 g).

Structure Determinations. Experimental data for compounds **5b**, **6**, **7d**, and **8** are reported in Table 4. Diffracted intensities for **6** and **8** were collected at 173(2) K on an Enraf-Nonius CAD4 diffractometer using Mo Kα X-radiation ($\lambda = 0.71073$ Å). Data were corrected for Lorentz and polarization effects, after which

numerical absorption corrections based on the measurement of the various crystal faces were applied.

A sphere of X-ray intensity data for **5b** was collected at 100(2) K on a Bruker SMART CCD area-detector diffractometer equipped with a rotating anode source (Cu Kα radiation, $\lambda = 1.54184$ Å). For several settings of φ, narrow data "frames" were collected for 0.3° increments of ω. Data for **7d** were acquired at 110(2) K using a Bruker-Nonius X8 Apex area-detector diffractometer (Mo Kα radiation). Several sets of data frames were collected at different θ values for various initial values of ϕ and ω, each frame covering a 0.5° increment of ϕ or ω. For the two data sets measured on area-detector devices, the data frames were integrated using SAINT;[36] the substantial redundancy in data allowed empirical absorption corrections (SADABS)[36] to be applied on the basis of multiple measurements of equivalent reflections.

The structures were solved (SHELXS-97) via conventional direct methods—with the exception of **7d**, which was solved using the Patterson function—and refined (SHELXL-97) by full-matrix least-squares on all F^2 data using SHELXTL, version 5.03 or 6.10.[36,37] All non-hydrogen atoms were assigned anisotropic displacement parameters. The locations of the cage carbon atoms were verified by examination of the appropriate internuclear distances and the magnitudes of their isotropic thermal displacement parameters.

All of the hydrogen atoms in organic functions were set riding on their parent atoms in calculated positions. The hydroxyl hydrogen in **7d** was located in difference maps, but upon being allowed positional refinement, it tended to collapse toward the parent O atom. Accordingly, this hydrogen was included riding on the oxygen atom, using a "rotating group" refinement that maximized the electron density at the calculated position (AFIX 147 card in SHELXL[37]). This calculated position was noted to correspond very closely to that initially obtained from difference maps and thus afforded a satisfactory treatment of this H atom. Cluster BH hydrogens in **6** and **8** were all located in difference maps, and their positions were successfully refined; those in **5b** and **7d** were set riding in calculated positions, apart from one of the hydrogen atoms [H(6)] involved in the agostic-type B−H ⇀ Pd interactions in **5b**, which was positionally refined. All hydrogen atoms were refined with fixed isotropic thermal parameters, calculated as $U_{iso}(H) = 1.2U_{iso}$(parent), except H(3) and H(6) in **5b**, whose temperature factors were freely refined.

Compounds **5b** and **8** each cocrystallize with two molecules of CH_2Cl_2 as solvate. One of these molecules in **5b** and both molecules in **8** were well-behaved and were treated as above. The other CH_2Cl_2 molecule in the asymmetric unit of **5b** was disordered, with the pair of Cl atoms located over two sites. For this molecule, the occupancies of the two parts were refined and then fixed at the ratio 60:40, and no hydrogen atoms were included.

Each molecule of **6** cocrystallizes with one molecule of CH_2Cl_2, as does each molecule of **7d**. In the solvate in crystals of **6**, one Cl atom was well-behaved, whereas the other was disordered over two sites. The two partial chlorines were assigned refining complementary occupancies, which were in the approximate ratio 86:14 at convergence. In **7d**, the pair of chlorides occupied two different sites. Thus, the molecule was refined as two parts, with only the carbon atom at a common site in each part. Refining complementary occupancies were assigned to each part, and these converged at the approximate ratio 75:25. For both of these solvates, separate methylene hydrogens were included in association with each part, and the solvate atoms were otherwise treated as described above.

Acknowledgment. We thank the Robert A. Welch Foundation, the E.P.S.R.C., and the National Science Foundation (M.R.I. Program, Grant CHE-0321214) for support.

Supporting Information Available: Full details of the crystal structure analyses in CIF format. This material is available free of charge via the Internet at http://pubs.acs.org.

IC048345W

(36) *APEX 2*, version 1.0-5, Bruker AXS: Madison, WI, 2003.
(37) SHELXTL, versions 5.03 and 6.10; Bruker AXS: Madison, WI, 1995 and 2000.